Influence of Acrylonitrile–Butadiene–Styrene (ABS) Morphology and Poly(styrene-*co*-acrylonitrile) (SAN) Content on Fracture Behavior of ABS/SAN Blends

Roberto S. Yamakawa, Carlos A. Correa,* Elias Hage, Jr.

Materials Engineering Department, Universidade Federal de São Carlos, Via Washington Luis, Km 235, 13565-905, São Carlos/SP, Brazil

Received 27 December 2002; accepted 31 December 2003

ABSTRACT: This study attempted to correlate morphological changes and physical properties for a high rubber content acrylonitrile–butadiene–styrene (ABS) and its diluted blends with a poly(styrene-*co*-acrylonitrile) (SAN) copolymer. The results showed a close relationship between rubber content and fracture toughness for the blends. The change of morphology in ABS/SAN blends explains in part some deviations in fracture behavior observed in ductile–brittle transition temperature shifts. © 2004 Wiley Periodicals, Inc. J Appl Polym Sci 92: 2606–2611, 2004

Key words: blending; mechanical properties; morphology; toughness; structure–property relations

INTRODUCTION

Acrylonitrile–butadiene–styrene terpolymers are a very important class of thermoplastics generically named as ABS. They are composed of a two-phase rubber-toughened plastic with a continuous poly(styrene-*co*-acrylonitrile) (SAN) copolymer glassy phase containing droplets of a dispersed polybutadiene latex. ABS morphology is primarily defined *in situ* during the manufacturing process that can be either in bulk or emulsion polymerization. The latter is mostly used industrially because it yields a fine graft control and a small submicron particle size distribution, which is more efficient for toughening the SAN matrix. On the other hand, the bulk polymerization yields a coarse multiple inclusion particle size that is ineffective for toughening ABS. Industrially manufactured ABS grades typically have 25% acrylonitrile in the SAN phase and a rubber particle size within the range 0.1–1 μm. The acrylonitrile polar groups provide a highly cohesive and very tough SAN matrix. Thus, the rubber-toughening mechanism in ABS is a combination of crazing and shearing depending on the load conditions. The main factors defining ABS morphology are as follows[1,2]:

- SAN composition and molecular weight
- Type of rubber, usually polybutadiene, ethylene propylene diene monomer rubber (EPDM, for acrylonitrile-EPDM rubber-styrene terpolymer [AES]), or polyacrylate rubbers (for acrylonitrile-styrene-acrylated rubber terpolymer [ASA])
- Rubber phase volume fraction
- Rubber particle size and particle internal structure
- Rubber crosslink density

In emulsion polymerization, the size distribution of the rubber particles is determined by the type and concentration of the emulsifying agent. The final rubber particle size is defined by latex agglomeration techniques that in some cases are convenient for presenting a bimodal distribution of agglomerates and individually dispersed rubber particles. The importance of a dual particle size distribution in the rubber-toughening process has also been highlighted for high-impact polystyrene/polystyrene (HIPS/PS) blends.[3] The particle size in such systems can be expressed either by statistical distributions of the particle diameters or by the interparticle distance (IPD).[4]

In ABS, the optimum average particle size for a good balance in stiffness, toughness, and surface gloss is within the range of 0.3–0.5 μm, whereas the IPD should vary within a lower range of 0.04–0.12 μm as a function of the manufacturing process.[5,6]

The use of ABS as an impact modifier for thermoplastics, particularly engineering plastics, by melt blending is largely used within the industry. Some of the examples that can be outlined are poly(vinyl chloride)/ABS,[7] bisphenol-A polycarbonate/SAN,[8–11] ny-

**Present address:* Universidade Sao Francisco, Itatiba-SP, Brazil.

Correspondence to: E. Hage, Jr. (elias@power.ufscar.br).

Contract grant sponsor: FAPESP (Brazil).

Contract grant sponsor: PRONEX/FINEP/CNPq (Brazil).

Journal of Applied Polymer Science, Vol. 92, 2606–2611 (2004)

TABLE I
ABS and SAN properties

Polymer	Chemical composition (%) AN	PBd	STy	Grafting (%)	Molar mass (Da)	$\bar{M}_w/\bar{M}_n$	Residual monomers (ppm)
ABS H300-L	12[a]	55[b]	32[c]	60	—	—	354
FREE SAN	17[a]	—	83[c]	—	$\bar{M}_n$ = 28,000 $\bar{M}_w$ = 64,000	2.26	—
SAN CN77E	25[a]	—	75[c]	—	$\bar{M}_n$ = 46,000 $\bar{M}_w$ = 110,000	2.39	—

[a] Values obtained by CHNS–O elemental analysis.
[b] Values obtained by Wijs method (iodine tritation).
[c] Values obtained by exclusion.

lon-6/ABS,[12,13] poly(butylene terephthalate)/ABS[14–20] and poly(propylene oxide)/ABS.[21] The fracture behavior of such blends may involve rather complex toughening mechanisms compared to those found in some rubber-toughened plastics such as HIPS, RTPMMA, and rubber-toughened polyolefins. For a better understanding of the role played by ABS as impact modifier it is necessary to change its phase morphology and observe the influence on the fracture behavior.

In this work, a high rubber content ABS grade was diluted by addition of increasing amounts of a SAN copolymer. The main purpose of the blending was to identify changes in toughening mechanisms related to the rubber phase dilution of the ABS with SAN, as well as the influence of the changes in phase morphology of the blend. The mechanical characterization was carried out by tensile and impact tests at various temperatures and by determination of the fracture parameter J_{Ic}.

The ABS morphology was characterized by transmission electron microscopy (TEM) with subsequent image analysis to quantify the average particle size and phase volume fraction. Plots of volumetric changes obtained in uniaxial tensile tests were used to distinguish dilatational (crazing) from constant volume (shearing) toughening mechanisms.

EXPERIMENTAL

Materials

The materials used in this work were an ABS terpolymer (coded H-300L), with a rubber content (polybutadiene) of 55% by weight and a grafting ratio of 0.6 by weight, and a SAN copolymer (coded CN77E); with an acrylonitrile content of 25% by weight, both from Bayer Polímeros S.A. (Brazil). The SAN CN77E (hereafter called SAN) is a special grade of SAN copolymer used for dilution of high rubber content ABS. Characteristics of both materials are summarized in Table I.

Mechanical blending

In the first step, the materials were molten and fed into a torque rheometer (Haake, Bersdorff, Germany) to determine the limiting blending conditions for the mixtures. The ABS/SAN compositions were previously prepared in a B&P 19-mm twin-screw extruder (Saginaw, MI), at 200°C and 130 rpm.

The specimens used for mechanical testing were injection molded at 220°C. The specimen dimensions were according to ASTM standards.

Mechanical characterization

The fracture toughness of ABS and ABS/SAN blends was characterized by Izod impact testing, according to ASTM D-256, and by three-point bending tests according to the ASTM D-6068 (J-integral method). Uniaxial tensile tests were performed in accordance with ASTM D-638.

Morphological characterization

Samples for the TEM analysis were obtained by ultracryomicrotomy at −60°C and a nominal thickness of 30 nm. The microtomed sections were stained in a 2% osmium tetroxide solution to promote a better contrast between the rubbery and the rigid phases. The images obtained by TEM were analyzed in the image analyzer, Quantimet Q600 (Leica, Wetzlar, Germany).

RESULTS AND DISCUSSION

Morphology of ABS terpolymer and ABS/SAN blends

Figure 1(a) shows a TEM micrograph for the parental ABS terpolymer, which has high rubber content (i.e., above 50% by weight). The phase morphology shows a dark stained rubbery phase and a thermoplastic SAN unstained phase, which seems to be dispersed, as a bright phase. The high degree of grafting on the ABS probably led to that morphology during melt-blending and injection-molding processes. Figure 1(b) shows different morphologies as SAN was blended with ABS. Thus the matrix becomes a SAN-rich phase (bright) with dispersed rubbery particles (dark). The change in morphology occurred as a result of the

addition of the free SAN molecules to the ABS, thus lowering its overall graft content.

Mechanical and rheological characterization

The tensile stress at yield (σ_y) follows the behavior observed by Kim and Shin,[22] where the yield stress decreases with increasing rubber content (Table II). The rubbery particles under hydrostatic stress may cavitate and trigger the matrix-toughening mechanism, thereby allowing the material to yield at lower tensile stress levels. According to Bucknall and coworkers[23,24] the yield stress level can be correlated to the rubber particle size and the rubber crosslink density. The stiffness of the blends increased with increasing amounts of SAN, as monitored through the tensile modulus behavior shown in Table II. This behavior was already expected, given that the SAN phase is much stiffer than the rubbery phase.

Interestingly, the results obtained from Izod impact testing tended to a maximum in the impact strength as a function of the SAN content added to ABS. The upper values in the impact strength occurred for mixtures with 40 to 50% of SAN, behavior that is probably attributable to the change in the morphology of ABS by addition of the SAN copolymer. The addition of 60 wt % of SAN into the blend yielded the impact strength close to that of the original ABS, with an excellent stiffness/toughness balance. For mixtures above 70% of SAN, it was noticed that the effect of dilution of the rubber content significantly reduced the impact strength. In other words, the rubber content should not be enough to toughen the ABS matrix. Rink and collaborators[25] reported for ABS a rubber content value of 20% by weight as the lowest bound to achieve acceptable impact strength levels. The ABS/SAN blend containing 70% of SAN shows an approximate rubber content of 16.5% by weight, which is lower than the value cited above. As expected, the torque rheometer results showed a decrease in the ABS viscosity with the addition of the SAN because it presents a much lower viscosity than that of the rubbery and grafted SAN phases.

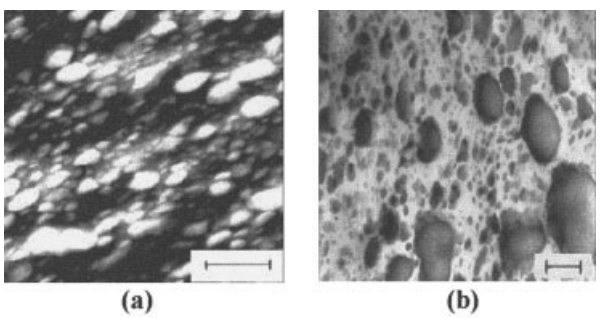

Figure 1 (a) TEM image of ABS morphology (scale bar = 1 μm). The bright particles represent the SAN-rich phase. (b) TEM image of the ABS/SAN blend morphology (scale bar = 0.2 μm). The dark particles represent the rubber-rich phase.

TABLE II
Mechanical Properties and Torque Rheometer Results

Added SAN (%)	Modulus (GPa)	σ_y (MPa)	Izod impact strenght (J/m)	Torque (220°C) (N m)
0	0.62	12.4	406	17.3
40	1.47	28.8	454	8.5
50	1.77	35.0	451	7.1
60	2.14	41.4	402	5.9
70	2.56	47.8	218	4.8
100	3.87	—	9.6	2.7

Analysis of the materials morphologies from TEM

Quantitative image analysis of TEM micrographs showed a bimodal rubber particle size distribution, as seen in Figure 1(b). The dual particle size distribution can be better observed if the particle size data are partitioned into two histograms, as depicted in Figure 2, for blends with 40 wt % of SAN. That was the main reason that the data of average rubber particle diameter and the correspondent volumetric fractions were presented separately as two populations in Table III. Population 1 corresponds to the particles with smaller size and also with lower volumetric fractions. On the other hand, population 2 corresponds to particles with larger size and also with larger volumetric fractions. It should be emphasized that population 2 is more likely to be responsible for ABS toughness.

Bucknall, Baer, and Parsons, followed by Kim and Shin,[22] all observed that rubber toughening is strongly dependent on the particle size of the dispersed phase. Particle diameters less than 0.3 μm are reported to be ineffective in the toughening process because they are unable to concentrate stress and/or cavitate and release the stored strain energy into the glassy matrix.

Population 1 presents a distribution with a high concentration of very small particles, which theoretically are not able to cavitate and concentrate stress. Therefore, that particle size population cannot take part in the toughening process. In spite of their large numbers, these particles correspond to a very small volumetric fraction in relation to population 2 (ϕ_2 in Table III).

Fracture toughness evaluation

Figure 3 shows the fracture mechanics parameter J_{Ic} as a function of the amount of SAN in the ABS/SAN blend. The fracture energy parameter J_{Ic} presents a maximum at 60% of SAN (i.e., rubber content around 22% by weight). Bernal and collaborators[26] also calcu-

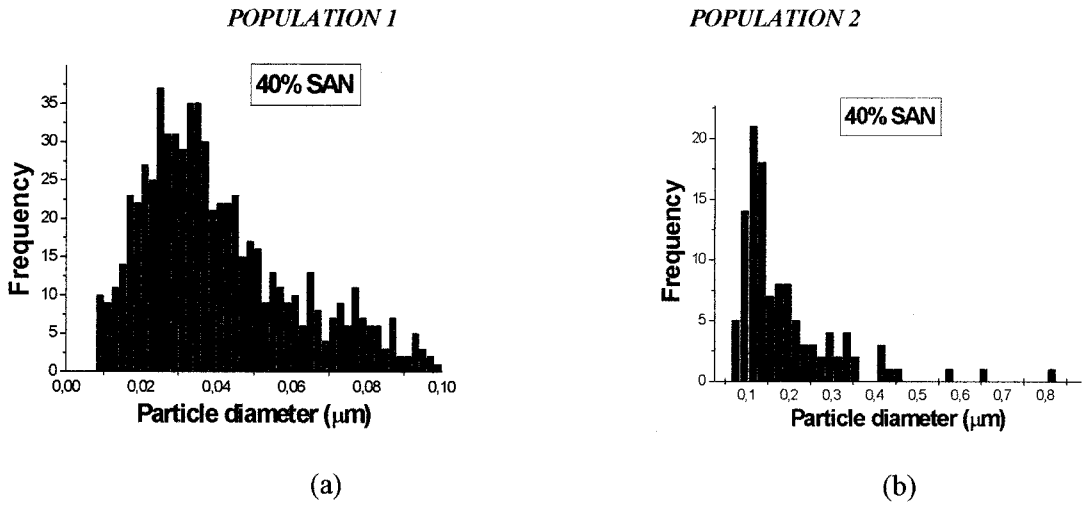

Figure 2 Distribution of particle diameters in the 60ABS/40SAN blend: (a) Population 1; (b) Population 2.

lated fracture energy for ABS with different rubber content and they found similar values within the range of 4.5 to 5.9 kJ/m^2. However, they found a maximum for the J_{Ic} value for an ABS at 15.5% by weight of rubber. The difference between both rubber content in ABS to achieve a maximum in the J_{Ic} value is probably attributable to the blend method used to disperse the rubber phase. In the present work the final rubber content in the blend was attained by melt mixing a high rubber content ABS with SAN, whereas in the former reference the rubber content was attained *in situ* during ABS polymerization.

Figure 4 shows a shift of the ductile–brittle transition (DBT) temperature toward higher temperatures as the rubber content is decreased. The shift in DBT is fitted reasonably well to an exponential decay.

Another surprising observation was the fracture behavior of parental ABS, which presented an increase in impact strength with decreasing temperatures, achieving a maximum value that was followed by a steep decrease. This behavior is different from that of the mixtures, where the impact strength decreases steadily with decreasing temperatures, and abruptly when it approaches its DBT temperature. The behavior for the high rubber content ABS was also reported by Hage and collaborators,[18] but without further comments. A possible explanation for that behavior may be related to the unusual morphology presented by the material (Fig. 1), where the rubber phase appears as an unusual continuous polybutadiene matrix. Therefore, the increase in the impact strength can be related to the increase of the Young's modulus and yield stress of the rubbery phase simultaneously at low temperatures. They should both be responsible for the increase on the required load to the yield process. Thus, the steep decrease in impact strength at lower temperatures occurs because the rubbery phase has reached its DBT temperature.

TABLE III
Average Particle Diameters and Volume Fraction of the Rubbery Phase Obtained by Quantitative Image Analysis of TEM Micrographs for the ABS/SAN Mixtures

% SAN	D_1 (μm)	D_2 (μm)	ϕ_1 (%)	ϕ_2 (%)
40	0.2	0.04	39	7
50	0.2	0.04	31	8
60	0.2	0.03	20	11
70	0.2	0.03	19	7

Toughening mechanisms

As observed in Table II, the average rubber particle diameter does not show a significant change with the addition of SAN into the ABS/SAN blends within the range 40–70% SAN. Therefore the change in the

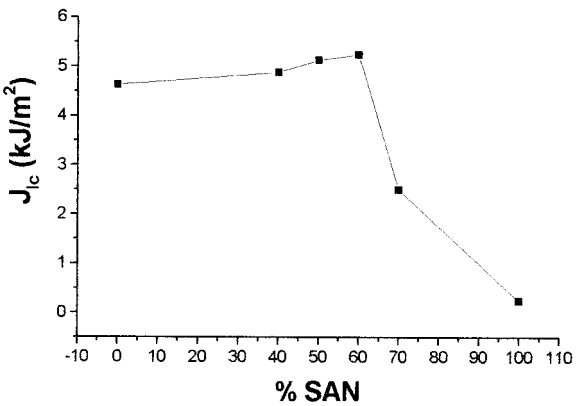

Figure 3 J_{Ic} as a function of the SAN amount added to the ABS/SAN blend.

toughening behavior of these materials depends on other parameters apart from the particle size. Finally, measurements of volumetric changes in uniaxial tension showed that increasing SAN content in the blend produces a shift from shearing characteristics of the high rubber content ABS to a larger contribution of dilatation mechanisms such as crazing and cavitation, as depicted in Figure 5.

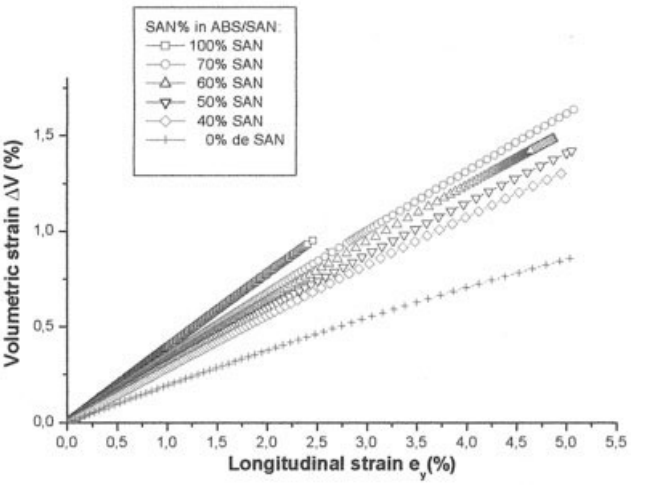

Figure 5 Volumetric strain changes as a function of axial deformation in ABS/SAN blends at varying SAN content.

CONCLUSIONS

ABS/SAN blends, containing parental high rubber content ABS with a phase morphology consisting of a polybutadiene continuous matrix, were investigated. The morphology changes by SAN addition were correlated with the fracture behavior of the ABS/SAN blend under impact tests, mainly at subambient temperatures. It was found that the incorporation of SAN into ABS led to a conventional rubber-toughened plastic morphology, that is, a rigid SAN matrix with dispersed rubbery particles rich in polybutadiene.

Structure–property relationships between morphological parameters and mechanical properties for ABS/SAN blends allowed some important conclusions on the ABS fracture behavior to be drawn. Actually, ABS toughness seemed to be strongly dependent on rubber content. Changes in toughening mechanisms from shearing to dilatation with increasing SAN content in the blend were also observed.

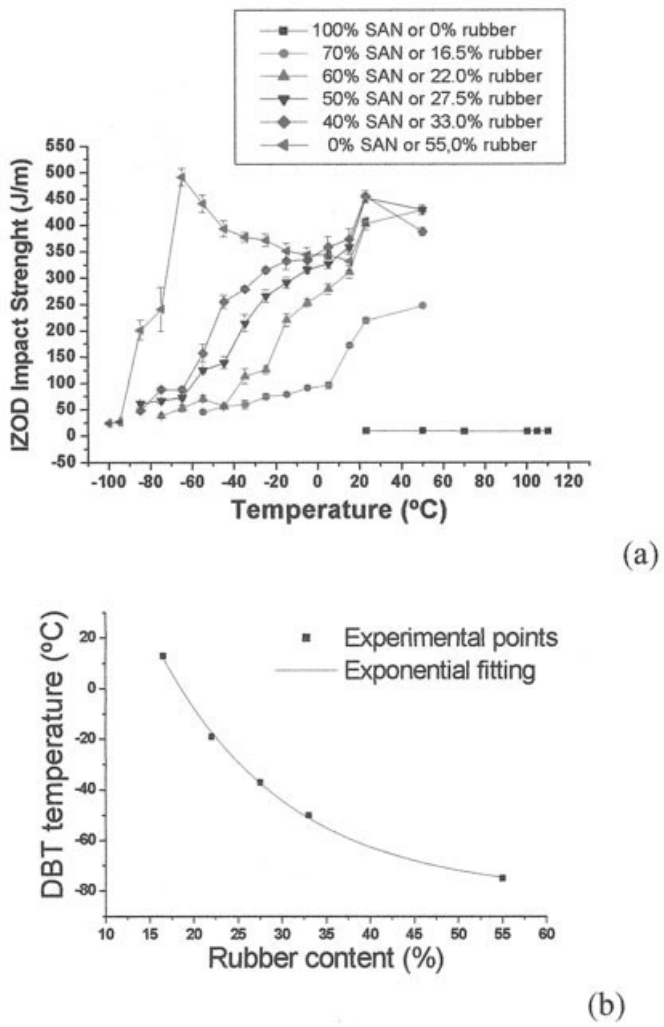

Figure 4 (a) Izod impact strength as a function of temperature and rubber content to obtain the ductile–brittle transition temperatures. (b) Ductile–brittle transition as a function of the rubber content.

The authors thank Bayer Polímeros S.A. (Brazil) for supplying the materials used for this study, Nitriflex S.A. for assistance in materials characterization, and the Brazilian research agencies FAPESP and PRONEX/FINEP/CNPq for financial support. The authors also thank Prof. Clive Bucknall for his important suggestions and contributions for the manuscript.

References

1. Bucknall, C. B. Toughened Plastics; Applied Science: London, 1977.
2. Echte, A. In: Rubber Toughened Styrene Polymers; Riew, C. K., Ed.; Rubber Toughened Plastics; Advanced Chemistry Series 222; American Chemical Society: Washington, DC, 1989.
3. Correa, C. A.; Sousa, J. A. J Mater Sci 1997, 32, 6539.
4. Wu, S. Polymer 1985, 26, 1855.
5. Haaf, F.; H.; Breuer, A.; Echte, B. J.; Schmitt, J Stabenow, J Sci Ind Res 1981, 40, 659.
6. Castellani, L.; Frassine, R.; Pavan, A.; Rink, M. Polymer 1996, 37, 1329.
7. Jin, D. W.; Shon, K. H.; Kim, B. K.; Jeong, H. M. J Appl Polym Sci 1998, 70, 705.
8. Greco, R.; Iavarone, M. Polym Eng Sci 2000, 40, 1701.
9. Wildes, G.; Keskkule, H.; Paul, D. R. J Polym Sci Polym Phys Ed 1999, 37, 71.

10. Tjong, S. C.; Meng, Y. Z. Eur Polym Mater 2000, 36, 123.
11. Yang, K. M.; Lee, S. H.; Oh, J. M. Polym Eng Sci 1999, 39, 1667.
12. Wildes, G.; Keskkula, H.; Paul, D. R. Polymer 1999, 40, 7089.
13. Kudva, R. A.; Keskkula, H.; Paul, D. R. Polymer 1998, 39, 2447.
14. Jang, P. S.; Kim, D. Polym Eng Sci 2000, 40, 1635.
15. Hale, W. R.; Pessan, L. A.; Keskkula, H.; Paul, D. R. Polymer 1999, 40, 4237.
16. Hale, W. R.; Lee, J. H.; Keskkula, H.; Paul, D. R. Polymer 1999, 40, 3621.
17. Hale, W. R.; Keskkula, H.; Paul, D. R. Polymer 1999, 40, 3665.
18. Hage, E.; Hale, W.; Keskkula, H.; Paul, D. R. Polymer 1997, 38, 3237.
19. Hale, W. R.; Keskkula, H.; Paul, D. R. Polymer 1999, 40, 3353.
20. Basu, D.; Banerjee, A. J Appl Polym Sci 1997, 64, 1485.
21. Lee, C.-H.; Lee, S.-K.; Kang, S.; Yun, S.; Shoe, S. J Appl Polym Sci 1999, 73, 841.
22. Kim, B. K.; Shin, G. S. J Appl Polym Sci 1993, 48, 945.
23. Bucknall, C. B.; Ayre, D. In: Proceedings of the 10th International Conference on Deformation, Yield and Fracture of Polymers, Institute of Materials, London, 1997.
24. Bucknall, C. B.; Correa, C. A.; Soares, V. L.; Zhang, X. C. In Proc. 9th Intl. Conference on Deformation Yield and Fracture of Polymers, Cambridge, UK, 1994.
25. Rink, M.; Riccò, T.; Lubert, W.; Pavan, A. J Appl Polym Sci 1978, 22, 429.
26. Bernal, C. R.; Frontini, P. M.; Sforza, M.; Bibbó, M. A. J Appl Polym Sci 1995, 58, 1.